GPS Occultation Density Observations Associated with the Midnight Temperature Maximum

Rebecca L. Bishop[1], Timothy Brubaker[2], and Paul R. Straus[1]

[1]The Aerospace Corporation
2310 E. El Segundo Blvd.
El Segundo, CA 90245-4609
USA

[2]Pennsylvania State University
University Park
State College, PA 16801
USA

ABSTRACT

The C/NOFS satellite, launched April 16, 2008, contains a GPS receiver that performs routine occultation measurements. The C/NOFS Occultation Receiver for Ionospheric Sensing and Specification, CORISS, measures total electron content (TEC) along the line-of-sight between C/NOFS and occulting GPS satellites. CORISS observes over 300 occultations per day in the low to mid latitude region. Within the low latitude thermosphere region exists the Midnight Temperature Maximum (MTM) phenomenon that is characterized by a significant increase in temperature and pressure, as well as a decrease or reversal in the meridional neutral winds. This persistent feature has a latitude variation [Colerico and Mendillo, 2002]. In this paper we report on global TEC enhancements that may be coincident with the MTM and discuss the coupling between the changing temperatures and wind to ionospheric dynamics.

1. INTRODUCTION

The Earth's Ionosphere is a dynamic region that, like all other atmospheric regions, cannot be studied in isolation. The plasma interacts with the neutral particles of the thermosphere, both chemically (primarily below 140 km) and dynamically. It is only by understanding the coupling of the ionosphere to various regions that we can truly understand ionospheric dynamics and variability. One such example is the Midnight Temperature and Density Maximums (MTM & MDM) of the thermosphere and its coupling to the ionospheric plasma as observed through the Midnight Density Maximum (MD_pM).

The MTM has been observed by ground-based and satellite-based sensors. The Neutral Atmosphere Temperature Instrument (NATE) on the Atmosphere Explorer-E satellite provided one of the earliest observations of the MTM [*Spencer et al.*, 1979; *Herrero and Spencer*, 1982]. The NATE set of observations first showed the latitudinal variation vs. local time of the MTM at 250 and 300 km altitude [*Herrero and Spencer*, 1982]. Accelerometer data from the CHAMP and San Marco III/V observed the thermospheric Midnight Density Maximum globally [*Ruan et*

al., 2014; *Arduini et al.*, 1996; *Arduini et al.*, 1997]. The CHAMP observations (2002-2009) showed that the MDM primarily occurs in a band within 20° of the geographic equator, similar to MTM observations [*Ruan et al.*, 2014]. Over the years there have been a number of MTM and MDM observations from ground-based sensors such as photometers, Fabry-Perot Interferometers (FPI), and incoherent scatter radars [e.g. *Colerico and Mendillo*, 2002; *Meriwether et al.*, 2008; *Oliver et al.*, 2012; *Hickey et al.*, 2014]. These studies, although limited to fixed locations, have provided insight into MTM formation and evolution. The Arequipa FPI observed a northward flow with a peak velocity of 30 m/s preceding the MTM maximum of ~200 K by 1.5-2 hours [*Meriwether et al.*, 2008]

The MD_pM has not been measured as thoroughly as its thermosphere counterparts. NmF2 nighttime enhancements, which can be considered an indication of an overall F-region MD_pM, were studied utilizing the extensive historical database of ionosonde measurements from around the world [*Farelo et al.*, 2002; *Maruyama et al.*, 2008]. In the *Farelo et al.* [2002] study, over 200,000 station-nights of data extending from 1955 to 1998 were used to show the geomagnetic latitude variation and seasonal dependence of nighttime NmF2 enhancements. MD_pM has also been observed using both ground-based and space-based GPS receivers. *Olwendo et al.* [2012] observed the strongest MD_pM signature during December solstice period. GPS radio occultation (GPSRO) measurements from the COSMIC satellites over a December solstice period (6 Nov 2006 to 5 Feb 2007) during quiet geomagnetic condition have shown MD_pM that vary in latitude and longitude [*Luan et al.*, 2008].

In the following paper, we utilize GPSRO observations from a low-inclination satellite to investigate the global nightly and seasonal variation, as well as altitude extent.

2. C/NOFS MISSION AND CORISS SENSOR

The Communication/Navigation Outage Forecast System (C/NOFS) satellite was launched on 4 April 2008 into an initial elliptical orbit of 405 x 853 km at an inclination of 13.0°. The C/NOFS satellite, an Air Force Research Laboratory, hosted six sensors: the Planar Langmuir Probe (PLP), the Coupled Ion Neutral Dynamics Investigation (CINDI) suite consisting of a neutral wind meter and ion velocity meter, the Vector Electric Field Instrument (VEFI), the Coherent Electromagnetic Radio Tomography (CERTO) beacon, and the C/NOFS Occultation Receiver for Ionospheric Sensing and Specification (CORISS). The purpose of the mission was to investigate equatorial ionospheric instabilities, their formation, evolution and decay. Specifically, plasma depletions (Equatorial Spread-F), and scintillation is of particular interest. A more complete description of the sensors and mission can be found in *de La Beaujardière et al.* [2004] and *de La Beaujardière et al.* [2009].

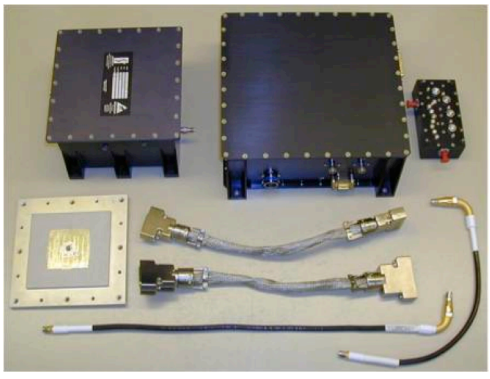

Figure 1. C/NOFS Occultation Receiver for Ionospheric Sensing and Specification (CORISS) sensor hardware.

The CORISS sensor is a GPS receiver specifically designed to make ionospheric occultation measurements. CORISS is a BlackJack receiver originally designed by JPL that has been modified (with consultation from JPL) for the C/NOFS mission to primarily be used as an ionospheric sensor. The BlackJack receiver is well understood and has flown on a number of satellites including the CHAMP and SAC-C missions [*Kuang et al.*, 2001; *Hajj et al.*, 2004]. The CORISS sensor consists of the CORISS receiver, antenna, and associated cabling as shown in Figure 1. The antenna is a limb-viewing patch antenna on the anti-velocity side of the spacecraft. The receiver tracks transmitted signals from the GPS satellite constellation at the L1 (1.575 GHz) and L2 (1.228 GHz) frequencies. Signals are acquired as the C/NOFS satellite's orbital motion causes GPS satellites to drift into the CORISS field-of-view and then they are tracked until lost as the GPS satellites disappear behind the Earth. This is known as setting occultations. The data presented here are obtained from the occulting portion of each satellite track as defined when the line of sight from the C/NOFS satellite to a GPS constellation satellite has a negative elevation angle relative the C/NOFS local horizontal. CORISS obtains approximately 400 occultations/day.

The CORISS receiver measures the L1/L2 carrier phase and signal-to-noise-ratio (SNR) of the associated tracking loops. The receiver's operating mode is controllable in regards to sampling rates. The three sampling rates, 0.1 Hz, 1.0 Hz, or 50 Hz, (low, medium, high) can be set according to occultation geometry. For example, for standard total electron content measurements, the medium sampling rate is used for the occulting portion of the track, providing ~1-2 km vertical spacing of data samples. The 50 Hz high rate sampling is reserved to obtain scintillation measurements and is used during the night-time portion of the orbit. In this paper we focus on TEC measurements and thus utilize medium rate sampled data.

3. OBSERVATIONS

A subset of the CORISS data was used for this study. An 8-month data set, September 2009 through April 2010, encompasses two equinoxes and one solstice period during a geomagnetically quiet period. The dataset was examined for the occurrence of MD_pM events. TEC profiles were used and the data was limited to within +/- 45° geographic latitude, which encompassed the majority of the CORISS observations. The TEC data was filtered further by restricting the time period of interest to 2100 to 0300 LT and by removing any occultation that had amplitude scintillation (S_4) values greater than 0.05, ensuring clean TEC profiles.

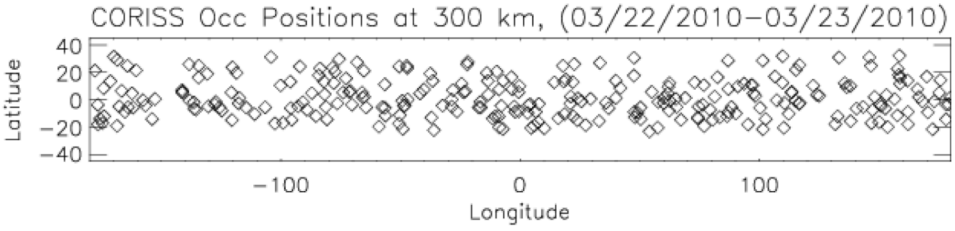

Figure 2. Illustration of CORISS observations over a 24-hour period distributed in longitude and limited to within +/- 45° latitude.

The location and time of the observations were referenced to the tangent point altitude 300 km unless otherwise specified. One of the challenges of working with GPSRO is distribution of observations. While GPSRO may provide relatively complete global coverage over a week or longer periods, a single LEO GPS receiver provides limited coverage at any particular longitude/latitude over a 24-hour period. Figure 2 shows the longitude and latitude coverage over a 24-hour period. Restricting the period to 2100 to 0300 LT reduces the observations to 35 over the entire globe. The number of observations varies depending on whether any ground contacts occur during the period.

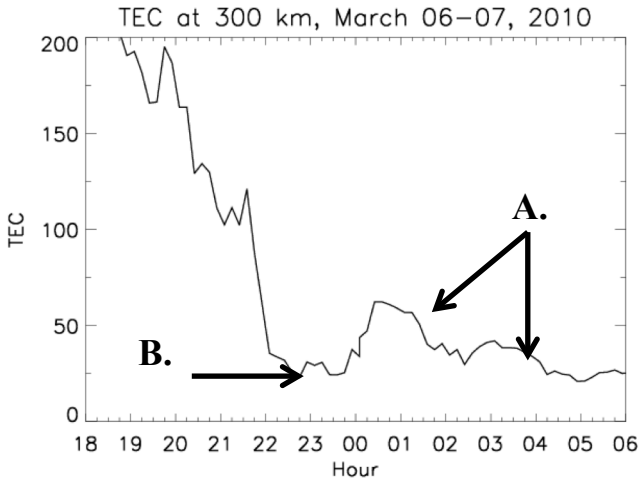

Figure 3. A collection of GPSRO TEC data for March 6-7 displaying nighttime density structures. The data shows two distinct post midnight peaks (A) and a possible pre-midnight peak (B).

Figure 3 shows an example of TEC values for a 12-hour period centered on midnight of 7 March 2010. This provides an illustration of the variation of TEC post the mid-day maximum through sunset and into the nightly density minimum. On this night a MD_pM event is clearly observed as indicated by the left A arrow. On this night there are two local density maximums. On most nights a local density minimum almost as great in magnitude as the overall nightly minimum is observed prior to the MD_pM (denoted by B in Figure 3). A week of nights with an MD_pM occurring almost nightly is shown in Figure 4.

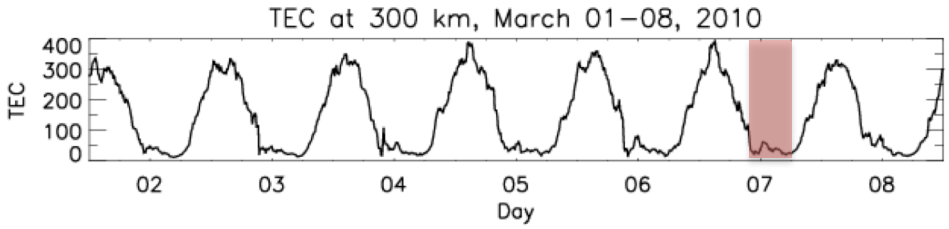

Figure 4. A week of CORISS TEC observations at a tangent point of 300 km between +/- 40° latitude. The highlighted area shows an MD_pM period along with local density minima. MD_pM are seen nearly every night during the period. The highlighted box indicates the data shown in Figure 3.

Although a 300 km tangent altitude is used as reference for determining location and time of MD_pM, we also examined other altitudes. This examination provided information on any altitude or temporal variation. Figure 5 show an example of the TEC versus local time at 25 km increments from 250 to 350 km. At all altitudes MD_pM is observed. The 250 and 275 km levels have the largest TEC values throughout the night and are nearly identical, indicating that the F-peak is within this altitude range for most of the evening. Above the F-peak nighttime TEC peak is visible for the remaining altitudes with magnitude of the MD_pM peak diminishing with increasing altitude. Another feature to note is the near convergence of all altitude TEC observations (20 TEC) post MD_pM (~4 LT).

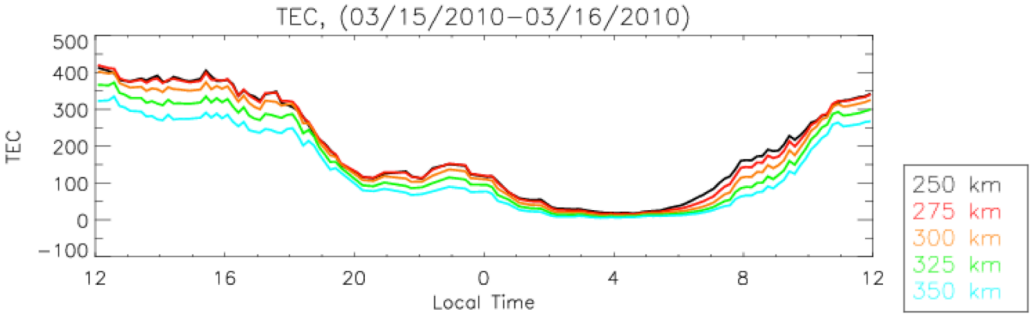

Figure 5. A single night showing TEC variation with local time as measured at various tangent point altitudes.

4. DISCUSSION

Eight months of GPSRO data from the CORISS sensor have shown that nighttime density enhancements (MD_pM) can be discerned using TEC profiles. Table 1 shows the MD_pM statistics during the period of interest. MD_pM appears to be an almost nightly occurrence occurring over 80% of the time. The TEC minimum and the peak density on average occur over approximately 80 min periods. Although MD_pM occurs nightly, the magnitude of the peak density enhancement can vary from night-to-night as observed in Figure 4. To determine the relative magnitude of the density changes, a polynomial fit is applied to 8 hours preceding the nightly TEC absolute minimum. The TEC profile is then subtracted from this baseline to provide the relative changes in TEC. An example is shown in Figure 6. On this night there appears to be two TEC density enhancements, similar to that observed in Figure 3. As seen by *Herrero and Spencer* [1982], the MTM peak local time varies with latitude. Since the data used to create Figure 6 spans +/- 45° latitude, the plot may be actually capturing multiple MD_pM occurring at different latitudes and/or longitudes. Regardless, this illustrates a periodicity to MD_pM occurrence, but whether it is temporal or spatial cannot be determined from this dataset.

2009-2010								
	Sept.	**Oct.**	**Nov.**	**Dec.**	**Jan.**	**Feb.**	**Mar.**	**Apr.**
Days of Data Available	27	30	29	29	25	27	28	29
Percentage of Nightly Occurrence	81.5	96.7	89.7	93.1	92.0	92.6	92.9	96.6
Approx. Average Time of First TEC Minimum (LT)	2115	2040	2120	2140	2200	2125	2130	2105
Approx. Average Time of Post-Sunset TEC Maximum (LT)	0105	2340	0035	0000	0045	2345	0005	0030

Table 1. MD_pM statistics over 8-month study period.

By the nature of GPSRO measurements, large horizontal areas of the ionosphere are sampled, often leading to smearing of features. However, *Luan et al.* [2008] showed that GPSRO MD_pM

observations agree with ionosonde data, confirming that observed MD_pM magnitudes are correct. Figure 6 shows TEC changes >40 TECU. MD_pM magnitudes are as low as 10 TECU. This night-to-night variation is expected since the MD_pM is formed through thermospheric coupling via MTM/MDM, which also varies within a large range, 25 to 175 K [*Meriwether et al.*, 2011].

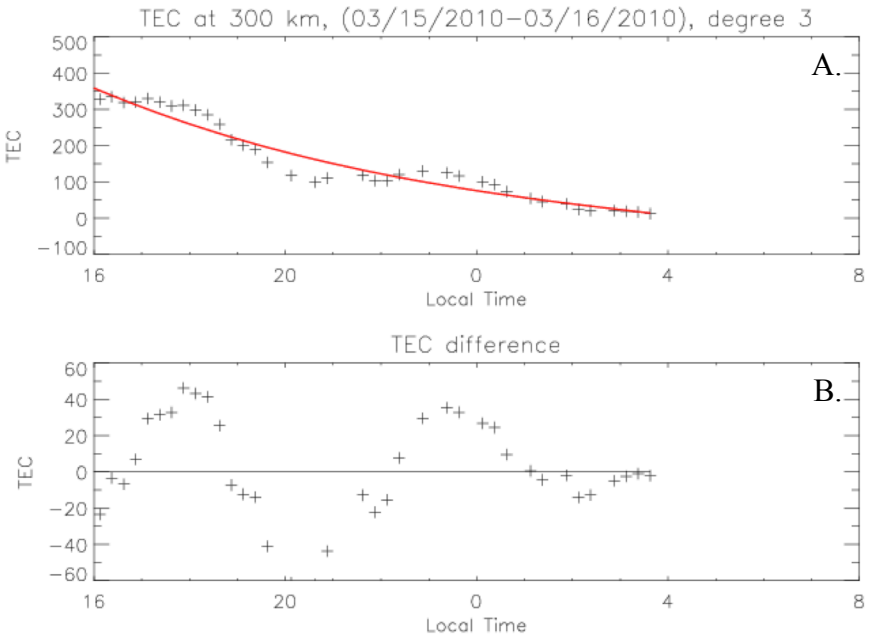

Figure 6. Panel A shows a polynomial fit to TEC over eight hours preceding night time minimum value. Panel B shows the difference between the fit and the actual data.

Recent modeling work has shown that the combination of a zonal wind due to the day-to-night pressure gradient combines with upward propagating tidal meridional wind to produce the MTM [*Akmaev et al.*, 2009, 2010]. AE-E observations showed the MTM first formed at the equator and then bifurcating to higher latitudes [*Herrero and Spencer*, 1982]. A similar latitude variation is observed in the CORISS data set. This MDM motion produces a reversal in the thermospheric meridional wind from the typical equatorward wind to a polar directed wind [*Meriwether et al.*, 2011]. The polar wind couples with the plasma, forcing it to lower altitudes along the magnetic field lines producing the enhance density. The MD_pM should have a similar variation in latitude with time, providing more evidence the dual enhancements observed in Figures 3 & 4 are due to latitude variations. By combining other GPSRO data sets with CORISS data, it may be possible to determine the exact longitude and latitude variations on a nightly rather than monthly basis.

5. CONCLUSIONS

The MD_pM is a distinct feature of the nighttime ionosphere that can be observed using GPSRO data. Because the C/NOFS mission is at a lower inclination, the majority of the GPSRO is located at low and mid latitudes. This study examined an 8-month period of GPSRO and observed several distinguishing characteristics. The density enhancement occurs nearly nightly with the lowest occurrence (~80%) during September 2009 and the highest occurrence (~96%) during April 2010. Preceding the MD_pM, a local density minimum is observed. On a global average the minimum occurs between 2100 and 2200 LT. Because of the large range of latitudes (+/- 45°) included in the dataset, 2-3 density enhancements are observed on a nightly basis. However, the average time of the peak MD_pM occurrence is between 2340 and 0045 LT. The peak MD_pM at 300 km ranges from ~10 TECU to more than 40 TECU from the background density. Finally, there is evidence that in addition to a density enhancement below the F-peak as noted in past studies, the MD_pM is observed to include at least 75 km above the F-peak.

Future investigations will expand this study to include multiple years of CORISS data supplemented with other GPSRO data sources. This will allow investigation on a nightly basis of the variation in MD_pM amplitude and occurrence as a function of latitude and longitude. Because it is clear that MD_pM results from coupling with thermospheric dynamics, a follow on study should examine a combination of global observations of the MTM/MDM and MD_pM.

ACKNOWLEDGEMENTS
This work was supported by The Aerospace Corporation's Technical Investment Program.

REFERENCES

Akmaev, R. A., Wu, F., Fuller-Rowell, T. J., & Wang, H. (2009). Midnight Temperature Maximum (MTM) in Whole Atmosphere Model (WAM) Simulations. Geophysical Research Letters, 36(L07108), doi:10.1029/2009GL037759.

Akmaev, R. A., Wu, F., Fuller-Rowell, T. J., Wang, H., & Iredell, M. D. (2010). Midnight Density and Temperature Maxima, and Thermospheric Dynamics in Whole Atmosphere Model Simulations. Journal of Geophysical Research, 115(A08326), doi:10.1029/2010JA015651.

Arduini, C., Laneve, G., & Ponzi U., (1996). The Midnight Density Maximum in the S. Marco V and the S. Marco III Equatorial Density Data Sets. Advances in Space Research, 18(9-10), 361-370.

Arduini, C., Laneve G., & Herrero, F. A., (1997). Local Time and Altitude Variation of Equatorial Thermosphere Midnight Density Maximum (MDM): San Marco Drag Balance Measurements. Geophysical Research Letters, 24(4), 377-380.

Colerico, M. J., & Mendillo, M. (2002). The Current State of Investigations Regarding the Thermospheric Midnight Temperature Maximum (MTM). Journal of Atmospheric and Solar-Terrestrial Physics, 64, 1361-1369.

de La Beaujardière, O., Jeong, L., Basu, M., Basu, S., Beach, T., Bernhardt, P., Burke, W., Groves, K., Heelis, R., Holzworth, R., Huang, C., Hunton, D., Kelley, M., Holzworth, R., Huang, C., Hunton, D., Kelley, M., Pfaff, R., Retterer, J., Rich, F., Starks, M., Straus, P., & Valladares, C. (2004). C/NOFS: A Mission to Forecast Scintillations. Journal of Atmospheric and Solar-Terrestrial Physics, 66, doi:10.1016/j.jastp.2004.07.030, 1573-1591.

de La Beaujardière, O., Retterer, J. M., Pfaff, R. F., Roddy, P. A., Roth, C., Burke, W. J., Su, Y. J., Kelley, M. C., Ilma, R. R., Wilson, G. R., Gentile, L. C., Hunton, D. E., & Cooke, D. L. (2009). C/NOFS Observations of Deep Plasma Depletions at Dawn. Geophysical Research Letters, 36(L00C06), doi:10.1029/2009GL038884.

Farelo, A. F., Herraiz, M., & Mikhailov, A. V. (2002). Global Morphology of Night-time NmF2 Enhancements. Annales Geophysicae, 20, 1795-1806.

Hajj, G. A., Ao, C. O., Iijima, B. A., & Kuang, D. (2004). CHAMP and SAC-C Atmospheric Occultation Results and Intercomparisons. Journal of Geophysical Research, 109(D06109), doi:10.1029/2003JD003909.

Herrero, F. A., & Spencer, N. W. (1982). On the Horizontal Distribution of the Equatorial Thermospheric Midnight Temperature Maximum and its Seasonal Variation. Geophysical Research Letters, 9(10), 1179-1182.

Hickey, D. A., Martinis, C. R., Erickson, P. J., Goncharenko, L. P., Meriwether, J. W., Mesquita, R., Oliver, W. L., & Wright, A. (2014). New radar observations of temporal and spatial dynamics of the midnight temperature maximum at low latitude and midlatitude. Journal of Geophysical Research Space Physics, 119, 10,499-10,506, doi:10.1002/2014JA020719.

Kuang, D., Bar-Sever, Y., Bertiger, W., Desai, S., Haines, B., Iijima, B., Kruizinga, G., Meehan, T., & Romans, L. (2001). Precise Orbit Determination for CHAMP using GPS Data from BlackJack Receiver. Proceedings of the 2001 National Technical Meeting of The Institute of Navigation, 762-770.

Luan, X., Wang, W., Burns, A., Solomon, S. C., & Lei, J. (2008). Midlatitude Nighttime Enhancements in F Region Electron Density From Global COSMIC Measurements Under Solar Minimum Winter Condition. Journal of Geophysical Research, 113(A09319), doi:10.1029/2008JA013063.

Maruyama, T., Saito, S., Kawamura, M., & Nozaki, K. (2008). Thermospheric Meridional Winds as Deduced from Ionosonde Chain at Low and Equatorial Latitudes and Their Connection with Midnight Temperature Maximum. Journal of Geophysical Research, 113(A09316), doi:10.1029/2008JA013031.

Meriwether, J., Faivre, M., Fesen, C., Sherwood, P., & Veliz, O. (2008). New Results on Equatorial Thermospheric Winds and the Midnight Temperature Maximum. Annales Geophysicae, 26, 447-466.

Meriwether, J. W., Makela, J. J., Huang, Y., Fisher, D. J., Buriti, R. A., Medeiros, A. F., & Takahashi, H. (2011). Climatology of the Nighttime Equatorial Thermospheric Winds and Temperatures Over Brazil Near Solar Minimum. Journal of Geophysical Research, 116(A04322), doi:10.1029/2011JA016477.

Oliver, W. L, Martinis, C. R., Hickey, D. A., Wright, A. D., & Amory-Mazaudier, C. (2012). A nighttime temperature maximum in the thermosphere above Saint Santin in winter. Journal of Geophysical Research, 117, doi:10.1029/2012JA017855.

Olwendo, O. J., Baki, P., Mito, C., & Doherty, P. (2012). Characterization of ionospheric GPS Total Electron Content (GPS-TEC) in low latitude zone over the Kenyan region during a very low solar activity phase. Journal of Atmospheric and Solar-Terrestrial Physics, 84-85, doi:10.1016/j.jastp.2012.06.003.

Ruan, H., Lei, J., Dou, X., Wan, W., & Liu, Y. C.-M. (2014). Midnight density maximum in the thermosphere from the CHAMP observations. Journal of Geophysical Research Space Physics, 119, 3741-3746, doi:10.1002/2013JA19566.

Spencer, N. W., Carignan, G. R., Mayr, H. G., Niemann, H. B., Theis, R. F., & Wharton, L. E. (1979). The Midnight Temperature Maximum in the Earth's Equatorial Thermosphere. Geophysical Research Letters, 6(6), 444-446.